An abundant quiescent stem cell population in *Drosophila* Malpighian tubules protects principal cells from kidney stones

Chenhui Wang and Allan C. Spradling

Howard Hughes Medical Institute Research Laboratories

Department of Embryology, Carnegie Institution for Science

3520 San Martin Dr.

Baltimore, Maryland 21218 USA

Author for correspondence (e-mail: spradling@carnegiescience.edu)

Running Head: Drosophila renal stem cells

Keywords: Malpighian tubule, kidney, kidney stone, stem cell, Drosophila, ureter, principal cell

Corresponding Author: Dr. Allan C. Spradling

Tel. 410-246-3015

Fax. 410-243-6311

Email: spradling@carnegiescience.edu

Summary

Adult *Drosophila* Malpighian tubules have low rates of cell turnover but are vulnerable to damage caused by stones, like their mammalian counterparts, kidneys. We show that *Drosophila* renal stem cells (RSCs) comprise a unique, unipotent regenerative compartment. RSCs respond only to loss of nearby principal cells (PCs), cells critical for maintaining ionic balance. Perhaps due to the large size of PCs they are outnumbered by RSCs, which replace each lost cell with multiple PCs of lower ploidy. RSCs share a developmental origin with highly active intestinal stem cells (ISCs), and like ISCs generate daughters by asymmetric Notch signaling, yet RSCs remain quiescent in the absence of damage. Nevertheless, the capacity for RSC-mediated repair extends the lifespan of flies carrying kidney stones. We propose that abundant, RSC-like stem cells exist in other tissues with low rates of turnover where they may have been mistaken for differentiated tissue cells.

Introduction

The *Drosophila* digestive system provides an outstanding model in which to identify novel mechanisms of tissue maintenance by stem cells (reviewed in Losick et al., 2011; Miguel-Aliaga et al., 2018). Highly active midgut intestinal stem cells (ISCs) produce regionally distinctive enterocytes and enteroendocrine cells throughout the midgut via asymmetric Notch signaling (Buchon et al., 2013; Dubreuil, 2004; Filshie et al., 1971; Marianes and Spradling, 2013; McNulty et al., 2001; Mehta et al., 2009; Shanbhag and Tripathi, 2009; Veenstra et al., 2008). Under normal conditions, ISCs respond to the demands of diet (O'Brien et al., 2011; Obniski et al., 2018), differences in spatial location (Buchon et al., 2013; Marianes and Spradling, 2013), mechanical forces (He et al., 2018; Li et al., 2018), the microbiota (Buchon et al., 2009a; Buchon et al., 2009b) and age (Biteau et al., 2008), all of which can influence the rate of cell turnover. In addition, ISCs support regenerative pathways that incorporate a broader range of cellular behavior when the digestive system is damaged by dietary toxins (Amcheslavsky et al., 2009; Chatterjee and Ip, 2009), or pathogens (Buchon et al., 2009a; Buchon et al., 2009b). Other regions of the gut are maintained and repaired in different ways. The hindgut lacks specialized stem cells and following damage is maintained primarily by induced polyploidization of post-mitotic epithelial cells (Cohen et al., 2018; Fox and Spradling, 2009; Losick et al., 2013; Sawyer et al., 2017).

The adult *Drosophila* excretory organ, the Malpighian tubules (MTs), comprise the fastest known fluid-transporting epithelium (Maddrell, 2009). MTs represent an anatomically simple adjunct of the digestive system consisting of initial, transitional, main and lower segments (Figures 1A and S1A). The four Malpighian tubules branch from two common ureters that drain into the gut at the midgut/hindgut junction. These tubular organs are essentially cellular

monolayers that function as kidneys and contain only two differentiated cell types, principal cells (PC) and stellate cells which are responsible for regulating ion balance and fluid secretion, respectively (Figures 1B and 1C; reviewed in Gautam et al., 2017).

MTs contain a distinct population of renal stem cells (RSCs) that express *escargot (esg)* (Singh et al., 2007) and arise from the same pool of adult midgut progenitors that generate posterior midgut ISCs (Takashima et al., 2013; Xu et al., 2018). RSCs are located both in the lower ureter, which develops from adult midgut progenitors, and in the upper ureter and lower segment of the Malpighian tubule (MT), which derive from the surviving larval ureter and larval MT (Takashima et al., 2013). RSCs were proposed to divide actively to produce daughter renoblasts (RBs) which migrate and endoreduplicate to replenish the two main MT cell types-principal cells (PCs) and stellate cells (SCs) located throughout the MT (Singh et al., 2007). Thus, Malpighian tubules are potential models for multiple aspects of metazoan kidney function, including the role of stem cells in maintaining adult nephric function.

Here we used novel methods to discover that RSCs comprise an abundant population of quiescent, unipotent stem cells that act only locally, on nearby principal cells. They respond to tissue injury located nearby, when they exit quiescence by upregulating the JNK, EGFR/MAPK and JAK/STAT pathways. Injury also activates asymmetric Notch signaling and upregulates Cut expression, to ensure that RSC daughters differentiate into replacement PCs. Replacement PCs produced by RSCs average about 8-fold lower ploidy than starting PCs, but are produced in a correspondingly greater number to maintain tissue DNA content. RSCs aid survival when Malpighian tubules are damaged by kidney stones, highlighting the importance of RSC-mediated regeneration.

Results

Adult Malpighian tubules contain abundant RSCs in the lower segment and ureter that decline in number during adulthood

Initially, we characterized the cell population in the ureter and lower tubules to quantitate the relative numbers of RSCs, and PCs. Interestingly, two populations of principal cells are easily distinguishable based on size and ploidy: small PCs (4-16C) are found in the lower ureter, and large PCs (32-128C) reside in the upper ureter and Malpighian tubules (Figures 1D and 1G). Both small PCs and large PCs express the homeobox protein Cut at high levels (Figures 1D1 and 1D2). We confirmed that *esg*-positive diploid cells are present only in the ureter and lower tubule (which we term "the stem cell zone"). The diploid cells contain many fewer mitochondria with fewer cristae than PCs (Figure 1C). Intriguingly, the esg^+ progenitor cells make up about 66% of cells in the stem cell zone (SCZ), more than the sum of small and large PCs (Figures 1D and 1F). We also detected a low expression level of Cut in esg^+ stem cells (Figures 1D2 and 1E), consistent with a recent study (Xu et al., 2018). We found that the esg^+ cell population slowly declines in number during adulthood (Figure 1H).

RSCs resemble ISCs in gene expression

To investigate the gene expression in the cells of the ureter and lower tubule, especially RSCs, we performed single cell RNA-seq to profile the transcriptome of disassociated tubule cells from the isolated ureters and lower tubules of young wild type female flies. 726 cells were captured and sequenced. The median genes that were recovered per cell is 1,662. We used Seurat (Butler et al., 2018) to do cell cluster assignment and four major and two minor cell clusters were resolved as shown in the t-Distributed Stochastic Neighboring Embedding (tSNE) plot

(Figure 2A). The four major cell groups correspond to RSCs (group 1) and three principal cell subtypes (group 2-4) based on expression of known markers (Figures 2B and 2C).

RSCs were assigned to group 1 cells based on the enriched expression of *esg*. Further analysis revealed that group 1 cells expressed many genes such as *Delta, Notch,* and *Sox21a* that are important for ISC regulation, and antibodies specific for Dl and Notch labeled RSCs (Figures 2D, 2E and 2G). Although both Dl and Notch are present in esg^{+} RSCs, Notch signaling activity was barely detectable in the adult Malpighian tubules, but readily detectable in midgut (Figure 2F), using a Notch signaling reporter construct expressing GFP under a Notch response element (NRE-GFP) (Saj et al., 2010).

By comparing transcription factor expression in group 1 RSCs with published data for ISCs to gain potential insight into cell identity (Dutta et al., 2015), we found that RSCs were strikingly similar to ISCs. Relatively highly expressed TFs in RSCs were *esg*, *Sox21a*, *E(spl)malpha-BFM*, *E(spl)mbeta-HLH*, *E(spl)m3-HLH*, *Sox100B*, *bun*, *zfh2*, *fkh*, *peb*, *Myc*, *Eip93F*, *Pdp1*, *Eip75B*, and *CrebA*. All of these genes are also expressed in ISCs. The chromatin decondensation factor 31 (*Df31*), which is associated with the establishment of open chromatin (Schubert et al., 2012), is highly enriched in RSCs (Figure 2H) and is also strongly expressed in ISCs (Dutta et al., 2015) (FlyGut-seq, http://flygutseq.buchonlab.com/), suggesting RSCs and ISCs share similar chromatin states.

Subtypes of principal cells in the SCZ

The principal cells (PC1-PC3) were assigned to clusters 2-4 based on the high expression of known principal cell marker genes including *ct*, *Alp4, Uro* and *salt* (Sozen et al., 1997; Stergiopoulos et al., 2009; Wallrath et al., 1990; Wang et al., 2004). PCs also expressed *NaPi-T*, *Eglp2*, *Vha100-2* and *ZnT35C*, genes involved in ion transport. The gene *caudal* (*cad*), which

encodes a homeobox domain transcription factor essential for normal hindgut formation (Wu and Lengyel, 1998), was also expressed in the PC1-PC3 cells (Figures 2C and 2I). As further validation, a Gal4 enhancer trap line derived from the *caudal* (*cad)* gene specifically labeled principal cells in the ureter and the lower tubules (Figure 2I). Further analysis of differentially expressed genes among clusters 2-4 revealed that they correspond to PC subtypes. The relatively lower expression of *Alp4* and *cad* in PC1 cells suggested they are the principal cells in the distal lower tubules and proximal main segments, whose principal cells highly express *Uro* and *salt* (Stergiopoulos et al., 2009; Wallrath et al., 1990). The differential expression of *Pvr* between PC2 and PC3 cells enabled us to tell them apart (Figure 2C). A Pvr-GFP reporter construct was highly expressed in the principal cells of the lower ureter (Figure S1C). Thus PC3 cells correspond to the small principal cells in the lower ureter, whereas PC2 cells correspond to the large principal cells in the upper ureter and proximal lower tubules.

Renal stem cells replenish principal cells in the SCZ but do not replenish stellate or principal cells in the upper tubules

In animals, tissue resident stem cells produce differentiated cells to maintain tissues in normal and/or stress conditions. To determine whether RSCs can respond to principal cell loss in the SCZ, we genetically ablated PCs by conditionally drive the expression of the apoptosis-inducing genes *reaper* and *hid* (Zhou et al., 1997). Forced expression of *UAS-hid, UAS-rpr* for 7 days at 29^{o}C with *c507-Gal4, tub-Gal80^{ts}*, which is a Gal4 enhancer trap line of Alp4 and specifically marks PCs in the SCZ (Figure S1D)(Yang et al., 2000), led to nearly complete ablation of preexisting large PCs in the SCZ. The regenerating SCZ was infiltrated with supernumerary small cells (Figures 3A and 3B). However, after 21 days of recovery at 18 ^{o}C, most small cells were gone and cells that were present appeared to be new PCs with high

expression levels of Cut (Figures 3C, S2A and S2B). Notably, the replacement PCs have significantly smaller nuclei compared to preexisting PCs in the lower tubules (Figure 3D).

It was previously reported that RSCs are multipotent stem cells that can replenish both principal cells and stellate cells throughout the Malpighian tubules (Singh et al., 2007). Since the upper tubules, which are about 1.5 mm long and are completely devoid of RSCs, we questioned whether RSCs can respond to tubule epithelial cell loss in the distal tubules. To investigate, we genetically ablated stellate cells or principal cells in the upper tubules using Gal4/UAS/Gal80^{ts} system to conditionally drive the expression of the apoptosis-inducing genes *reaper* and *hid*, and then monitored regeneration at 18^{o}C to minimize further expression.

We first examined whether stellate cells which are only localized in the upper tubules could be replaced. Previous studies have shown that stellate cells express the zinc-finger transcription factor *teashirt* (*tsh*) (Denholm et al., 2003; Sozen et al., 1997). Consistently, both the Gal4 enhancer trap line (*tsh*^{md621}) and the lacZ enhancer trap line (*tsh*^{04319}) specifically label stellate cells in Malpighian tubules (Figure S2C). Expression of *UAS-hid, UAS-rpr* with *tsh-Gal4, tub-Gal80*^{ts} for 7 days at 29^{o}C resulted in a near-complete ablation of stellate cells (Figures S2D, S2E and S2G). However, we did not observe any replenishment of stellate cells even 30 days after shifting the animals back to 18^{o}C for recovery (Figures S2F and S2G). This result indicates that stellate cells are not replaced in adult flies and that RSCs do not respond to stellate cell loss.

We next investigated whether RSCs can respond to the loss of principal cells in the upper tubules. The *Gal4* under the control of putative promoter of *Uro* (referred as *Uro-Gal4*) is specifically expressed in the principal cells in the main segment (Terhzaz et al., 2010), as revealed by the expression *UAS-myrRFP* driven by *Uro-Gal4*, no expression was detected in stellate cells (Figure S2H). We ablated principal cells in the main segment by expressing *UAS-*

hid, UAS-rpr with *Uro-Gal4, tub-Gal80^{ts}*. After expressing *rpr* and *hid* 7 days at 29^{o}C, most principal cells in the main segment were ablated (data not shown). After shifting the animals back to 18^{o}C for recovery, we observed supernumerary ectopic tubule cells at the distal end of the stem cell zone. However, the ectopic tubule cells never migrated into the upper tubule to replace lost principal cells in the upper tubules (Figure S2I). These results indicate that RSCs may sense and respond to damage located very close to the SCZ, however, newly generated RSC daughters do not migrate into the upper tubules. Collectively, these results demonstrated that RSCs can replenish the PCs in the SCZ but lack detectable capacity to replenish stellate cells and PCs in the upper tubules.

Damaged PCs within the SCZ are replaced by smaller cells

One characteristic of the new PCs generated in response to PC loss was a reduction in size. For example, when PCs in the SCZ were ablated by expression of *rpr* and *hid* for 7 days followed by recovery at 18 ^{o}C for 21 days, nearly all the giant polyploid PCs were lost (Figures 2A-C). New PCs were generated throughout the SCZ that were about eight-fold lower in nuclear volume (Figure 3D).

To determine how sensitive RSCs are to the loss of principal cells in the Malpighian tubule, we developed a surgical procedure that allows the distal ends of Malpighian tubules to be severed in a living adult animal after pulling it through a small incision in the abdominal cuticle (Figure 3E, METHOD DETAILS). The cut end appears to close off and the operated animals remain viable and live a normal lifespan. When the cut end was located within the SCZ, DNA replication as measured by 5- ethynyl-2′-deoxyuridine (EdU) incorporation increased in nearby *esg*-positive RSCs, but not throughout the entire SCZ (Figure 3F). Damage in the main segment could only activate RSCs if it was close to the SCZ junction. Damage about five PCs away

increased EdU incorporation in the most distal RSCs of the SCZ (Figure 3G). However, damage about ten PCs away did not increase EdU-labelled RSCs (Figure 3H), indicating it failed to activate RSCs. This suggests that RSCs sense damage through short range signals extending less than ten cells away along the tubule.

We investigated repair at the cellular level by lineage marking RSCs using esg-GAL4 and GAL80^{ts} (see METHOD DETAILS). Cutting a tubule within the SCZ and activating lineage tracing by temperature shift revealed a substantial increase in the number of RSC daughters (i.e. marked *esg*$^{-}$) cells near the surgical site (Figures 3I and 3I'), indicating that local RSCs were induced to generate *esg*$^{-}$ daughters by surgical injury in the SCZ. In contrast, truncating the tubule within the main segment about 10 PCs away from the SCZ did not elicit any production of lineage-marked *esg*$^{-}$cells in the SCZ (Figures 3J and 3J').

Damage activates quiescent RSCs via upregulation of multiple short range signaling pathways

To investigate what damage-induced signals activate the RSCs, we examined damage pathways known to activate ISC proliferation. Extensive studies have shown that the EGFR/MAPK, Jak/Stat, Wnt, Hippo, PVF, JNK, Insulin, and BMP pathways are all involved in eliciting ISC division either under steady state conditions or during regeneration following cellular damage (Gervais and Bardin, 2017; Guo et al., 2016; Jiang et al., 2016; Li and Jasper, 2016). Reporters for four of these pathways, JNK, Jak/Stat, MAPK and Yki pathways were induced upon surgical injury (Figure S3). Interestingly, the JNK pathway was induced as early as 12-24h after injury in cells at the surgical site as revealed by the expression of *UAS-GFP driven by puc*^{E69}*-Gal4 (Adachi-Yamada, 2002)*, regardless of whether the surgical site was within the SCZ or in the distal upper tubules (Figure S3A). However, upregulation of Jak/Stat and EGFR

pathway reporters took place in RSCs close to the surgical site, which was only within the SCZ or in the proximal upper tubules, as assayed by the expression of 10XStat92E-GFP (Bach et al., 2007) and dpERK (Gabay et al., 1997), respectively (Figures S3B and S3C). *Diap1-lacZ* , which is widely used as reporter of Yki activity (Huang et al., 2005), was also induced in cells near the surgical site within the SCZ (Figure S4D), suggesting the Yki signaling was activated. JNK pathway activation can induce the expression of *Drosophila* Jak/Stat pathway ligands (Upd1, Upd2 and Upd3), which in turn transduce Jak/Stat signaling in neighboring cells (Jiang et al., 2009). We propose that RSCs are activated by damage-induced JNK activation, which is then relayed by short range signals including Upds and EGFs. This mechanism may explain why only local damage is sufficient to activate RSCs.

Notch signaling is essential to generate differentiated RSC progeny

We next investigated the genes responsible for controlling the differentiation of replacement principal cells from activated RSCs. As in the case of ISCs, Notch signaling was found to play a critical and central role. Notch signaling was barely detectable in RSCs under normal conditions using NRE-GFP as a reporter (Figure 4A). However, Notch activity was induced in cells close to the surgical site after MT resection (Figure 4A). Expression of Cut, a transcription factor that distinguishes renal from midgut tissue (Xu et al., 2018), was also elevated in the RSCs near the surgical site (Figure 4B).

In the midgut, disruption of Notch blocks intestinal stem cell daughter differentiation and leads to the proliferation of ISC-like cells (Ohlstein and Spradling, 2007). In the SCZ, we found that RNAi-mediated knockdown of Notch caused an accumulation of RSC-like cells near the surgical site (Figures 4C and 4D). To further validate the finding, heat-shock induced N^{55e11} mutant clones marked by GFP were generated using MARCM system in animals that had been

fed with the nephrotoxic drug allopurinol (Lee and Luo, 1999). Wild type RSCs clones typically consisted of multiple Cut^+ replacement principal cells along with one or more Dl^+ RSCs (Figures 4E and 4G). In contrast, N^{55e11} mutant RSCs failed to upregulate Cut and polyploidize to form replacement principal cells. Instead they continued to produce cells expressing Dl (Figures 4F and 4H). These observations suggest that upon damage, RSCs can divide asymmetrically and activate the Notch pathway in one daughter cell, which turns on Cut and differentiates into an RB, a precursor that subsequently differentiates into principal cell.

Consistent with this model, forced expression of the Notch intracellular domain (NICD), a constitutively active form of Notch using *esg-Gal4*^{ts} while tagging RSCs with esg>RFP caused depletion of esg>RFP^+ cells after 14 days shifted to 29^{o}C. The depletion of esg>RFP^+ cells was not due to cell death, as they were still expressing lineage marker (Figures S4A-B). *ct* is a well-known Notch target (Sun and Deng, 2005) that has been suggested to play an important role in renal differentiation and to be expressed in RSCs at low levels (Xu et al. 2018). We noticed that Cut expression was upregulated in regenerating cells in the lower tubule after surgery, suggesting that its upregulation might promote replacement PC production (Figure 4B). Indeed, expression of *UAS-ct* with *esg-Gal4*^{ts} recapitulated the NICD-caused depletion of esg$^+$ cells (Figure S4C). In addition, forced expression of *ct* or forced expression of NICD in RSCs caused them to differentiate towards small replacement PCs expressing Alp4 (Figures S4D-F). Thus as in ISCs, Notch signaling is required and sufficient for RSC differentiation. However, unlike differentiating midgut cells, PCs require the upregulation of *ct* in RSC daughters (Figure 4I).

RSCs can switch between symmetric and asymmetric division after injury

The large increase in diploid renal cells that accompanies regeneration of multiple PCs raised the question of how multiple PC progenitors (RBs) arise. In particular, RBs could all be

produced by repeated asymmetric divisions of RSCs, or they could be expanded by symmetric divisions of already formed RBs. RBs are Notch-induced and can be labeled by NRE-GFP. We first examined which cell types undergo mitotic division in the regenerating Malpighian tubules. Following expression of *rpr* and *hid* with *c507-Gal4*^{ts} for 7 days, mitoses were readily detected. All phospho-Histone H3 (PH3)-marked mitotic cells were also positive for Dl and negative for NRE-GFP (Figures 5A-B). These data demonstrate that RSCs are the only cells that divide after injury in the adult Malpighian tubules.

Replacement cells could be produced using fewer divisions if RSCs divided symmetrically to expand in number, before or in concert with asymmetric divisions to produce new RBs. Previous studies have shown that ISCs can switch between symmetric and asymmetric modes to adapt to the physiological stimuli (O'Brien et al., 2011). We thus investigated the division mode of RSCs following acute injury elicited by surgery. Using the twin-spot MARCM system (Yu et al., 2009), we induced twin-spot MARCM clones 1 day after surgical damage to the Malpighian tubules. Twin-spot MARCM system allowed us to label both daughter cells with permanent lineage markers GFP or RFP after heat-shock induced mitotic recombination. By examining the clone-forming capacity of the labelled daughter pairs, we infered the individual fates of labelled daughter cells and thus determined whether they were produced by symmetric or asymmetric division of their mother stem cell (Figure 5C). On day 4-7 after clone induction, we observed both symmetric lineages and asymmetric lineages in the SCZ. Approximately 70% of twin spots (n=46) were derived from RSC/RSC pairs since both RFP-marked clone and GFP-marked clone had multiple cells (Figures 5D-F). Interestingly, all RSC/RSC pairs were observed at the surgical sites, where the replacement cells were most urgently required. In addition the RSC closer to the surgical site usually gave rise to more cells

than its sibling RSC did (Figures 5D and 5E-E1). The RSC/RB pairs, which gave rise to approximately 30% of examined twin spots, were localized several PCs away from surgical sites (Figures 5E and 5E2). These results show that RSCs employ symmetric as well as asymmetric divisions to generate replacement PCs.

Renal stem cells are normally quiescent

We examined the expression of the mitotic marker PH3 among RSCs labeled by esg>RFP in order to estimate the frequency of RSC division in the absence of injury. No mitotic cells were observed in wild-type Malpighian tubules (n=47) under normal conditions (Figures 6A and 6C), in contrast to previous claims (Singh et al., 2007). However, 10.7 ± 5.1 (mean ± SD, n=18) mitotic cells on average were seen per pair of Malpighian tubules after expression of esg>*upd1* in RSCs for 7 days. EdU incorportion over 2d was used as a more sensitive system to detect RSC division under normal conditions. EdU incorporation in midgut cells was widespread within this interval, reflecting the high stem cell activity in this tissue (Figure 6D). However, very few RSCs (~0.3%) were labeled in the same period (Figures 6D-6E). After 4d of labeling, EdU incorporation could be detected in only about 1% of RSCs (Figure 6E). We conclude that RSCs are unlike ISCs and do not actively maintain renal cells in the absence of injury causing cell loss.

The Fly-FUCCI system was used to assess the cell cycle phase distribution of RSCs (Zielke et al., 2014). Fly-FUCCI is based on combination of fluorochrome-tagged degrons from the Cyclin B and E2F1 proteins, which are degraded during mitosis or S phase (Figure S5A), respectively. Expression of *UAS-CFP-E2F1*$_{1-230;}$*UAS-Venus-CycB*$_{1-266}$ driven in RSCs by *esg-Gal4,UAS-myrRFP* showed that 42% of RSCs (n=461 cells analyzed) expressed both *CFP-E2F1*$_{1-230}$ and *Venus-CycB*$_{1-266}$ and had a 4C DNA content, indicative of G2 phase. Only 3.2% of

RSCs expressed *Venus-CycB$_{1-266}$* but not *CFP-E2F1$_{1-230}$*, consistent with the low percentage of RSCs in S phase revealed by EdU incorporation. 9.8% of RSCs expressed *CFP-E2F1$_{1-230}$* but not *Venus-CycB$_{1-266}$*, indicative of G1 phase. Interestingly, 47% of esg>RFP^{+} RSCs expressed neither *CFP-E2F1$_{1-230}$* nor *Venus-CycB$_{1-266}$*, suggesting these cells lack expression of cell cycle progression factors (Figures 6F and S5B). In addition, the cells double negative for E2F1 and CycB have a 2C DNA content (Figure S5C), characteristics of G0 state (Cheung and Rando, 2013). Taken together, these data indicated that the vast majority of RSCs are arrested at G2 or G0 phase under non-stress conditions.

Renal stem cells are unipotent

To further study the behavior of RSCs, we used the MARCM system to permanently mark individual dividing RSCs and their progeny via heat-shock induced mitotic recombination (Lee and Luo, 1999). Without heat shock, we observed very sparse clones in midgut and Malpighian tubules, showing that the MARCM system was associated with little background clone induction (Figure 6G). After a low dose heat shock at 37^{o}C, a substantial number of clones were induced in the midgut reflecting the active ISC division in this tissue, but clones were not detected among quiescent RSCs of the Malpighian tubules (Figure 6H). However, 6 successive 1 hr heat shocks spaced 24 hours apart (6X hs) was found to induce RSC division (Figure 6I'), either because it damaged PCs and stimulated regeneration, or else over-rode the normal controls of RSC proliferation.

The induced MARCM clones were confined to the SCZ (Figure 6I), and none were observed in the upper tubules (N= 1957 clones, n>100 flies), indicating that they were generated by RSCs. We examined the cellular composition of these marked clones to probe the differentiation potential of RSCs. 7 days after clone induction, both single-cell clones and multi-

cell clones were detected. Single-cell clones comprise only one polyploid cell negative for Dl, as expected if the RB was marked following an asymmetric RSC division. In addition, multi-cell RSC clones were observed that consisted of one Dl^{+} 2C cell and several Dl^{-} polyploid cells (Figure 6K). Staining of Cut showed that the RSC clones comprise a 2C cell with low level expression of Cut and 2-4 polyploid cells expressing higher level of Cut that represent newly completed PCs derived from the RSC (Figure 6L). Notably, new principal cells derived from RSCs are 8-16c and never reach the ploidy of preexisting principal cells (64-128C).

Renal stem cells respond to injury caused by kidney stones

While protection from extreme heat stress provides one possible reason *Drosophila* kidneys contain RSCs, we also investigated another potential problem, cell loss caused by kidney stones (Figures 7 and S6). Xanthine stones in *Drosophila* Malpighian tubules (analogous to human hereditary xanthinuria) can be reproducibly generated by mutating the *rosy* (*ry*) gene, encoding xanthine dehydrogenase (XDH) (Figures S6A-C; (Bonse, 1967; Mitchell and Glassman, 1959), or by feeding adults the XDH inhibitor allopurinol (Figure S6D; (Chi et al., 2015). Although control flies did not show Malpighian tubule stones even after 14d, 80% or more of *ry* mutant adults contained stones in the SCZ within 1d of eclosion, and the stones grew in size over the next 4 weeks (Figure S6C). Stones appeared first in the ureter and lower tubules, but could eventually be found in more distal regions. Similar effects were observed in flies treated with allopurinol (Figure S6D). *ry* mutant Malpighian tubules with stones suffered a loss of nearby PCs due to detachment from the tubule epithelium and movement into the lumen, a process that frequently started near the junction of the lower segment with the ureter (Figures 7A-7D and S6B). In their place, many new small cells appeared, some of which showed evidence of polyploidization (Figure 7E). We noticed that the number of cells positively correlated with the

size of stones in the SCZ (Figures S6E-F), demonstrating that it is stone-induced damage activating RSCs to proliferate and replenish the SCZ.

Consistent with this notion, transcriptome profiling by mRNA-seq of dissected SCZ from ry^{506} mutants carrying stones revealed that many genes associated with mitotic cycling and RSC activation were increased relative to wild type (Figure S7A). In consonance with surgical injury studies, activation of the JNK, Jak/Stat, EGFR, Yki and Notch signaling were induced by stones as revealed by both mRNA-seq and reporter assays (Figure S7A-G).

Likewise, allopurinol treatment of wild type flies greatly increased the number of total cells, as well as esg^{+} cells in the SCZ that incorporate EdU (Figures S6G-H). *esg-Gal4*^{ts} directed Flp-out lacZ marked lineage tracing showed that the increased cells were derived from esg^{+} cells (data not shown). The distribution of cell cycle stages of RSCs in stone-carrying animals was different from those of RSCs in control animals (Figure S6I). The percentage of RSCs at G0 decreased from 47% to 4.6% (n=624 cells). In addition, the number of mitotic clones was significantly increased after Allopurinol treatment (Figures S6J-L). Molecular analysis of clones validated that RSCs give rise to daughter cells that differentiate into new principal cells as indicated by the high level expression of Cut (data not shown). However, clonal marking again showed that the RSC-generated cells did not replace distal PCs or migrate from the lower to the more distal regions of the Malpighian tubule (Figure S6M).

If esg^{+} cells are prevented from migrating into the SCZ by expressing a dominant negative form of Rac1 (Rac1.N17) during pupal development such that adults lack RSCs (Figure 7H, (Takashima et al., 2013), then few new small cells or polyploid PCs were produced after allopurinol treatment (Figure 7I). The lifetime of such RSC-depleted animals on allopurinol was significantly reduced compared to treated animals that retained their RSCs (Figure 7J). These

observations show that RSCs are required to generate new replacement PCs in response to damage and that RSC-mediated regeneration is advantageous for survival under the conditions of kidney stress.

Discussion

Reserved regenerative cells distribute to the regions of tissues that are targeted by injury

Adult stem cells are widely known to exist as rare cell populations in tissues and organs. Here we show that adult *Drosophila* RSCs are an exception. RSCs significantly outnumber the principal cells that they maintain, yet do not divide unless a neighboring principal cell is lost. Interestingly, these large RSC populations are confined to the ureter and lower tubules, and are not found throughout the Malpighian tubes. We observed that xanthine stones often start to form in the ureter and lower tubules, and frequently damage these regions, suggesting that the deployment of RSCs in the SCZ is driven by evolutionary selection pressure for regenerative capacity in regions where stones are most likely.

It has long been known that some parts of mammalian kidneys such as proximal tubule undergo cellular regeneration after acute kidney injury (AKI) (Witzgall et al., 1994). The S3 segment of proximal tubule is often damaged in cases of acute kidney injury elicited by ischemia, sepsis, trauma or other mechanisms (Lazzeri et al., 2019). However, it has been controversial as to whether tubular stem cells or progenitor cells contribute to regeneration. The long-standing idea is that the repair and regeneration of nephron tubules are predominantly based on the dedifferentiation of surviving tubular cells, which in turn divide to replace lost cells (Humphreys et al., 2011; Humphreys et al., 2008; Kusaba et al., 2014). However, tissue-resident tubular progenitor cells, which are more resistant to death, have recently been characterized and

demonstrated to play an important role in murine tubular regeneration (Angelotti et al., 2012; Kang et al., 2016; Lazzeri et al., 2018; Rinkevich et al., 2014). Thus, both *Drosophila* and mice employ reserved progenitor cells (RSCs in *Drosophila* or tubular progenitor cells in mice) to replenish specific cells in renal regions that are vulnerable to injury. We propose that RSC-like quiescent stem cells of limited potency exist in tissue regions that are preferential targets of injury, in multiple tissues with little or no normal cell turnover.

G0 and G2 arrest of adult *Drosophila* renal stem cells

Active stem cells such as intestinal stem cells and germline stem cells have been extensively studied in *Drosophila*. However, studies on *Drosophila* quiescent stem cells are just emerging (Boukhatmi and Bray, 2018; Chaturvedi et al., 2017; Otsuki and Brand, 2018). Although quiescent stem cells have been identified in many tissues, the characteristics of quiescent stem cells are still not well understood since they represent a very rare population in most tissues (Cheung and Rando, 2013; Li and Clevers, 2010). Adult *Drosophila* renal stem cells are abundant and comprise approximately 70% of total cells in the ureter and the tubule. Thus, *Drosophila* RSCs represent a favorable model to further understand quiescent stem cells.

Quiescent stem cells are commonly believed to arrest in G0/G1. RSCs, in contrast, were found to arrest in G0 (47%) or G2 (42%) (Figure 6F). Although it might appear to be counterintuitive, accumulating evidence shows that quiescent stem cells frequently arrest in G2. For instance, the majority of *Drosophila* neural stem cells become quiescent and are arrested in G2 phase for 24 h after embryogenesis (Otsuki and Brand, 2018). G2 arrest is essential to maintain postnatal muscle stem cells in zebrafish (Nguyen et al., 2017). We propose that the bimodal arrest observed for RSCs is advantageous since G2 RSCs would be well positioned to respond promptly to injury, while G0 RSCs could serve as long term reservoirs. Since RSCs

decline in number over time, it would be interesting to determine whether there is a selective change in the distribution of cell cycle phases.

Why are adult-derived PCs lower in ploidy than embryo-derived PCs

It is widely assumed that during regeneration, stem cells generate daughters that differentiate into identical replacement tissue, but RSCs generate replacement PCs of substantially lower in ploidy compared to preexisting PCs carried from the larva, in most of the SCZ. The final ploidy levels of both ISC and RSC progenitors are not entirely invariant, but usually remain within narrow limits. Daughter cells are sent on a course of differentiation via Notch signaling, and endocycles continue until a final tissue size is sensed. Likewise, in the *Drosophila* follicle cell lineage, mitotic divisions downstream from the stem cell continue until a mitotic to endocycle transition signals the onset of differentiation (Deng et al., 2001; Ohlstein and Spradling, 2007; Sun and Deng, 2005). If the number of cells differs from normal or changes during growth, the remaining cells will proliferate for a greater or lesser number of endocycles until the target tissue size is achieved (Deng et al., 2001; Edgar et al., 2014; Ovrebo and Edgar, 2018). Adult PCs are probably lower ploidy because the number of progenitor cells is relatively large so that many RBs are rapidly generated relative to the number of lost PCs. This arrangement speeds regeneration since it takes a smaller number of endocycles to achieve the starting tissue mass using a larger number of progenitors. In contrast, in the embryo when the Malpighian tubules initially form, PCs are established and start to endoreduplicate when the tissue is very small. Thereafter, growth of larval Malpighian tubules is completely driven by the continued endoreduplication rather than cell division.

RSCs may also generate replacement PCs of smaller size, because the enormous adult PCs carried over from the larva are less adapted to an adult organ than the smaller cells typical

for adult digestive tissues. The failure to replace the larval tubules during pupal development may be a physiological necessity for maintaining ionic and water balance during pupal development. Thus, repair to smaller size PCs during adulthood might provide a functional upgrade that completes the rebuilding of the tissue along the lines other tissues undergo during pupal development.

Modeling kidney stone disease in *Drosophila*

One common form of kidney diseases is kidney stone formation, whose incidence and prevalence have been increasing over the past several decades worldwide (Romero et al., 2010). While non-obstructing stones do not cause significant damages apart from hematuria, obstructing stones can elicit both acute as well as irreversible chronic kidney injury (Coe et al., 2005; Rule et al., 2011). Much remains to be learned about the cellular and molecular mechanisms underlying kidney stone formation. Type I Hereditary Xanthinuria in humans, which is caused by mutation of *xanthine dehydrogenase* (aka *xanthine oxidoreductase*, *XDH/XOR*), can damage kidney and even lead to renal failure (Akinci et al., 2013). Our data show that xanthine stones can cause sloughing of principal cells and shorten the lifespan of *Drosophila*. Additionally, RSC-mediated regeneration of the SCZ extends the lifespan. Our data demonstrate that *Drosophila* can be used to model kidney stone formation and help understand stone-induced damage and repair. Continued work on the formation and RSC-mediated repair of *Drosophila* stones is likely to provide new information relevant to the prevention and treatment of kidney stones.

STAR★ METHODS

Detailed methods are provided in Supplemental Material and include the following:

- KEY RESOURCES TABLE
- CONTACT FOR REAGENT AND RESOURCE SHARING
- EXPERIMENTAL MODEL AND SUBJECT DETAILS
    - *Drosophila* and husbandry
- METHOD DETAILS
    - Immunostaining and microscopy
    - Heat shock scheme for mosaic analysis
    - Electron microscopy
    - Surgical removal of *Drosophila* Malpighian tubules
    - Flip-out lacZ marked lineage tracing
    - Allopurinol feeding
    - Single cell RNA-seq
    - Bulk RNA-seq
    - Genetic cell ablation and recovery
    - X-Gal Staining
    - EdU incorporation
- QUANTIFICATION AND STATISTICAL ANALYSIS
    - Quantification of cell nuclear volume
    - Lifespan measurement
- DATA AND SOFTWARE AVAILABILITY SUPPLEMENTAL INFORMATION

Acknowledgements

We are grateful to Jennifer Urban & Xin Chen (Johns Hopkins University), the Bloomington *Drosophila* Stock Center (BDSC) , Vienna *Drosophila* Resource Center (VDRC) and Developmental Studies Hybridoma Bank (DSHB) for *Drosophila* strains and reagents. We thank Allison Pinder and Frederick Tan for assistance in RNA sequencing and analysis. We thank Joshua Blundon for assistance in collecting samples for single cell RNA-seq. We are grateful to Mike Sepanski for help in electron microscopy. We thank Steve DeLuca, Ethan Greenblatt, Robert Levis, and other members of the Spradling laboratory for providing comments on the manuscript.

AUTHOR CONTRIBUTIONS

C. W. and A.C.S. conceptualized the study and wrote the manuscript. C.W. performed all the experiments.

DECLARATION OF INTERESTS

The authors declare no competing interests.

REFERENCES

Adachi-Yamada, T. (2002). Puckered-GAL4 driving in JNK-active cells. Genesis *34*, 19-22.

Akinci, N., Cakil, A., and Oner, A. (2013). Classical xanthinuria: a rare cause of pediatric urolithiasis. Turk J Urol *39*, 274-276.

Amcheslavsky, A., Jiang, J., and Ip, Y.T. (2009). Tissue damage-induced intestinal stem cell division in Drosophila. Cell Stem Cell *4*, 49-61.

Angelotti, M.L., Ronconi, E., Ballerini, L., Peired, A., Mazzinghi, B., Sagrinati, C., Parente, E., Gacci, M., Carini, M., Rotondi, M*., et al.* (2012). Characterization of renal progenitors committed toward tubular lineage and their regenerative potential in renal tubular injury. Stem Cells *30*, 1714-1725.

Bach, E.A., Ekas, L.A., Ayala-Camargo, A., Flaherty, M.S., Lee, H., Perrimon, N., and Baeg, G.H. (2007). GFP reporters detect the activation of the Drosophila JAK/STAT pathway in vivo. Gene Expr Patterns *7*, 323-331.

Biteau, B., Hochmuth, C.E., and Jasper, H. (2008). JNK activity in somatic stem cells causes loss of tissue homeostasis in the aging Drosophila gut. Cell Stem Cell *3*, 442-455.

Bonse, A. (1967). [Studies on the chemical nature and formation of the urinary conglomerate in the Malpighian vessels of the rosy mutant of Drosophila melanogaster]. Z Naturforsch B *22*, 1027-1029.

Boukhatmi, H., and Bray, S. (2018). A population of adult satellite-like cells in Drosophila is maintained through a switch in RNA-isoforms. Elife *7* e35954.

Buchon, N., Broderick, N.A., Chakrabarti, S., and Lemaitre, B. (2009a). Invasive and indigenous microbiota impact intestinal stem cell activity through multiple pathways in Drosophila. Genes Dev *23*, 2333-2344.

Buchon, N., Broderick, N.A., Poidevin, M., Pradervand, S., and Lemaitre, B. (2009b). Drosophila intestinal response to bacterial infection: activation of host defense and stem cell proliferation. Cell Host Microbe *5*, 200-211.

Buchon, N., Osman, D., David, F.P., Fang, H.Y., Boquete, J.P., Deplancke, B., and Lemaitre, B. (2013). Morphological and molecular characterization of adult midgut compartmentalization in Drosophila. Cell Rep *3*, 1725-1738.

Buszczak, M., Paterno, S., Lighthouse, D., Bachman, J., Planck, J., Owen, S., Skora, A.D., Nystul, T.G., Ohlstein, B., Allen, A.*, et al.* (2007). The carnegie protein trap library: a versatile tool for Drosophila developmental studies. Genetics *175*, 1505-1531.

Butler, A., Hoffman, P., Smibert, P., Papalexi, E., and Satija, R. (2018). Integrating single-cell transcriptomic data across different conditions, technologies, and species. Nat Biotechnol *36*, 411-420.

Chatterjee, M., and Ip, Y.T. (2009). Pathogenic stimulation of intestinal stem cell response in Drosophila. J Cell Physiol *220*, 664-671.

Chaturvedi, D., Reichert, H., Gunage, R.D., and VijayRaghavan, K. (2017). Identification and functional characterization of muscle satellite cells in Drosophila. Elife *6*. e301107.

Cheung, T.H., and Rando, T.A. (2013). Molecular regulation of stem cell quiescence. Nat Rev Mol Cell Biol *14*, 329-340.

Chi, T., Kim, M.S., Lang, S., Bose, N., Kahn, A., Flechner, L., Blaschko, S.D., Zee, T., Muteliefu, G., Bond, N.*, et al.* (2015). A Drosophila model identifies a critical role for zinc in mineralization for kidney stone disease. PLoS One *10*, e0124150.

Coe, F.L., Evan, A., and Worcester, E. (2005). Kidney stone disease. J Clin Invest *115*, 2598-2608.

Cohen, E., Allen, S.R., Sawyer, J.K., and Fox, D.T. (2018). Fizzy-Related dictates A cell cycle switch during organ repair and tissue growth responses in the Drosophila hindgut. Elife *7* e38327.

Deng, W.M., Althauser, C., and Ruohola-Baker, H. (2001). Notch-Delta signaling induces a transition from mitotic cell cycle to endocycle in Drosophila follicle cells. Development *128*, 4737-4746.

Denholm, B., Sudarsan, V., Pasalodos-Sanchez, S., Artero, R., Lawrence, P., Maddrell, S., Baylies, M., and Skaer, H. (2003). Dual origin of the renal tubules in Drosophila: mesodermal cells integrate and polarize to establish secretory function. Curr Biol *13*, 1052-1057.

Dubreuil, R.R. (2004). Copper cells and stomach acid secretion in the Drosophila midgut. Int J Biochem Cell Biol *36*, 745-752.

Dutta, D., Dobson, A.J., Houtz, P.L., Glasser, C., Revah, J., Korzelius, J., Patel, P.H., Edgar, B.A., and Buchon, N. (2015). Regional Cell-Specific Transcriptome Mapping Reveals Regulatory Complexity in the Adult Drosophila Midgut. Cell Rep *12*, 346-358.

Edgar, B.A., Zielke, N., and Gutierrez, C. (2014). Endocycles: a recurrent evolutionary innovation for post-mitotic cell growth. Nat Rev Mol Cell Biol *15*, 197-210.

Filshie, B.K., Poulson, D.F., and Waterhouse, D.F. (1971). Ultrastructure of the copper-accumulating region of the Drosophila larval midgut. Tissue Cell *3*, 77-102.

Fox, D.T., and Spradling, A.C. (2009). The Drosophila hindgut lacks constitutively active adult stem cells but proliferates in response to tissue damage. Cell Stem Cell *5*, 290-297.

Gabay, L., Seger, R., and Shilo, B.Z. (1997). In situ activation pattern of Drosophila EGF receptor pathway during development. Science *277*, 1103-1106.

Gautam, N.K., Verma, P., and Tapadia, M.G. (2017). Drosophila Malpighian Tubules: A Model for Understanding Kidney Development, Function, and Disease. Results Probl Cell Differ *60*, 3-25.

Gervais, L., and Bardin, A.J. (2017). Tissue homeostasis and aging: new insight from the fly intestine. Curr Opin Cell Biol *48*, 97-105.

Guo, Z., Lucchetta, E., Rafel, N., and Ohlstein, B. (2016). Maintenance of the adult Drosophila intestine: all roads lead to homeostasis. Curr Opin Genet Dev *40*, 81-86.

He, L., Si, G., Huang, J., Samuel, A.D.T., and Perrimon, N. (2018). Mechanical regulation of stem-cell differentiation by the stretch-activated Piezo channel. Nature *555*, 103-106.

Huang, J., Wu, S., Barrera, J., Matthews, K., and Pan, D. (2005). The Hippo signaling pathway coordinately regulates cell proliferation and apoptosis by inactivating Yorkie, the Drosophila Homolog of YAP. Cell *122*, 421-434.

Humphreys, B.D., Czerniak, S., DiRocco, D.P., Hasnain, W., Cheema, R., and Bonventre, J.V. (2011). Repair of injured proximal tubule does not involve specialized progenitors. Proc Natl Acad Sci U S A *108*, 9226-9231.

Humphreys, B.D., Valerius, M.T., Kobayashi, A., Mugford, J.W., Soeung, S., Duffield, J.S., McMahon, A.P., and Bonventre, J.V. (2008). Intrinsic epithelial cells repair the kidney after injury. Cell Stem Cell *2*, 284-291.

Jiang, H., Patel, P.H., Kohlmaier, A., Grenley, M.O., McEwen, D.G., and Edgar, B.A. (2009). Cytokine/Jak/Stat signaling mediates regeneration and homeostasis in the Drosophila midgut. Cell *137*, 1343-1355.

Jiang, H., Tian, A., and Jiang, J. (2016). Intestinal stem cell response to injury: lessons from Drosophila. Cell Mol Life Sci *73*, 3337-3349.

Kang, H.M., Huang, S., Reidy, K., Han, S.H., Chinga, F., and Susztak, K. (2016). Sox9-Positive Progenitor Cells Play a Key Role in Renal Tubule Epithelial Regeneration in Mice. Cell Rep *14*, 861-871.

Kusaba, T., Lalli, M., Kramann, R., Kobayashi, A., and Humphreys, B.D. (2014). Differentiated kidney epithelial cells repair injured proximal tubule. Proc Natl Acad Sci U S A *111*, 1527-1532.

Lazzeri, E., Angelotti, M.L., Conte, C., Anders, H.J., and Romagnani, P. (2019). Surviving Acute Organ Failure: Cell Polyploidization and Progenitor Proliferation. Trends Mol Med *25*, 366-381.

Lazzeri, E., Angelotti, M.L., Peired, A., Conte, C., Marschner, J.A., Maggi, L., Mazzinghi, B., Lombardi, D., Melica, M.E., Nardi, S.*, et al.* (2018). Endocycle-related tubular cell hypertrophy and progenitor proliferation recover renal function after acute kidney injury. Nat Commun *9*, 1344.

Lee, T., and Luo, L. (1999). Mosaic analysis with a repressible cell marker for studies of gene function in neuronal morphogenesis. Neuron *22*, 451-461.

Li, H., and Jasper, H. (2016). Gastrointestinal stem cells in health and disease: from flies to humans. Dis Model Mech *9*, 487-499.

Li, L., and Clevers, H. (2010). Coexistence of quiescent and active adult stem cells in mammals. Science *327*, 542-545.

Li, Q., Nirala, N.K., Nie, Y., Chen, H.J., Ostroff, G., Mao, J., Wang, Q., Xu, L., and Ip, Y.T. (2018). Ingestion of Food Particles Regulates the Mechanosensing Misshapen-Yorkie Pathway in Drosophila Intestinal Growth. Dev Cell *45*, 433-449.

Liao, Y., Smyth, G.K., and Shi, W. (2014). featureCounts: an efficient general purpose program for assigning sequence reads to genomic features. Bioinformatics *30*, 923-930.

Losick, V.P., Fox, D.T., and Spradling, A.C. (2013). Polyploidization and cell fusion contribute to wound healing in the adult Drosophila epithelium. Curr Biol *23*, 2224-2232.

Losick, V.P., Morris, L.X., Fox, D.T., and Spradling, A. (2011). Drosophila stem cell niches: a decade of discovery suggests a unified view of stem cell regulation. Dev Cell *21*, 159-171.

Love, M.I., Huber, W., and Anders, S. (2014). Moderated estimation of fold change and dispersion for RNA-seq data with DESeq2. Genome Biol *15*, 550.

Maddrell, S. (2009). Insect homeostasis: past and future. J Exp Biol *212*, 446-451.

Marianes, A., and Spradling, A.C. (2013). Physiological and stem cell compartmentalization within the Drosophila midgut. Elife *2*, e00886.

McNulty, M., Puljung, M., Jefford, G., and Dubreuil, R.R. (2001). Evidence that a copper-metallothionein complex is responsible for fluorescence in acid-secreting cells of the Drosophila stomach. Cell Tissue Res *304*, 383-389.

Mehta, A., Deshpande, A., Bettedi, L., and Missirlis, F. (2009). Ferritin accumulation under iron scarcity in Drosophila iron cells. Biochimie *91*, 1331-1334.

Micchelli, C.A., and Perrimon, N. (2006). Evidence that stem cells reside in the adult Drosophila midgut epithelium. Nature *439*, 475-479.

Miguel-Aliaga, I., Jasper, H., and Lemaitre, B. (2018). Anatomy and Physiology of the Digestive Tract of Drosophila melanogaster. Genetics *210*, 357-396.

Mitchell, H.K., Glassman, E., and Hadorn, E. (1959). Hypoxanthine in rosy and maroon-like mutants of Drosophila melanogaster. Science *129*, 268-269.

Nguyen, P.D., Gurevich, D.B., Sonntag, C., Hersey, L., Alaei, S., Nim, H.T., Siegel, A., Hall, T.E., Rossello, F.J., Boyd, S.E., *et al.* (2017). Muscle Stem Cells Undergo Extensive Clonal Drift during Tissue Growth via Meox1-Mediated Induction of G2 Cell-Cycle Arrest. Cell Stem Cell *21*, 107-119.

O'Brien, L.E., Soliman, S.S., Li, X., and Bilder, D. (2011). Altered modes of stem cell division drive adaptive intestinal growth. Cell *147*, 603-614.

Obniski, R., Sieber, M., and Spradling, A.C. (2018). Dietary Lipids Modulate Notch Signaling and Influence Adult Intestinal Development and Metabolism in Drosophila. Dev Cell *47*, 98-111.

Ohlstein, B., and Spradling, A. (2007). Multipotent Drosophila intestinal stem cells specify daughter cell fates by differential notch signaling. Science *315*, 988-992.

Otsuki, L., and Brand, A.H. (2018). Cell cycle heterogeneity directs the timing of neural stem cell activation from quiescence. Science *360*, 99-102.

Ovrebo, J.I., and Edgar, B.A. (2018). Polyploidy in tissue homeostasis and regeneration. Development *145,* dev156034.

Pertea, M., Kim, D., Pertea, G.M., Leek, J.T., and Salzberg, S.L. (2016). Transcript-level expression analysis of RNA-seq experiments with HISAT, StringTie and Ballgown. Nat Protoc *11*, 1650-1667.

Rinkevich, Y., Montoro, D.T., Contreras-Trujillo, H., Harari-Steinberg, O., Newman, A.M., Tsai, J.M., Lim, X., Van-Amerongen, R., Bowman, A., Januszyk, M., *et al.* (2014). In vivo clonal analysis reveals lineage-restricted progenitor characteristics in mammalian kidney development, maintenance, and regeneration. Cell Rep *7*, 1270-1283.

Romero, V., Akpinar, H., and Assimos, D.G. (2010). Kidney stones: a global picture of prevalence, incidence, and associated risk factors. Rev Urol *12*, e86-96.

Rule, A.D., Krambeck, A.E., and Lieske, J.C. (2011). Chronic kidney disease in kidney stone formers. Clin J Am Soc Nephrol *6*, 2069-2075.

Saj, A., Arziman, Z., Stempfle, D., van Belle, W., Sauder, U., Horn, T., Durrenberger, M., Paro, R., Boutros, M., and Merdes, G. (2010). A combined ex vivo and in vivo RNAi screen for notch regulators in Drosophila reveals an extensive notch interaction network. Dev Cell *18*, 862-876.

Sawyer, J.K., Cohen, E., and Fox, D.T. (2017). Interorgan regulation of Drosophila intestinal stem cell proliferation by a hybrid organ boundary zone. Development *144*, 4091-4102.

Schubert, T., Pusch, M.C., Diermeier, S., Benes, V., Kremmer, E., Imhof, A., and Langst, G. (2012). Df31 protein and snoRNAs maintain accessible higher-order structures of chromatin. Mol Cell *48*, 434-444.

Shanbhag, S., and Tripathi, S. (2009). Epithelial ultrastructure and cellular mechanisms of acid and base transport in the Drosophila midgut. J Exp Biol *212*, 1731-1744.

Singh, S.R., Liu, W., and Hou, S.X. (2007). The adult Drosophila malpighian tubules are maintained by multipotent stem cells. Cell Stem Cell *1*, 191-203.

Sozen, M.A., Armstrong, J.D., Yang, M., Kaiser, K., and Dow, J.A. (1997). Functional domains are specified to single-cell resolution in a Drosophila epithelium. Proc Natl Acad Sci U S A *94*, 5207-5212.

Stergiopoulos, K., Cabrero, P., Davies, S.A., and Dow, J.A. (2009). Salty dog, an SLC5 symporter, modulates Drosophila response to salt stress. Physiol Genomics *37*, 1-11.

Sun, J., and Deng, W.M. (2005). Notch-dependent downregulation of the homeodomain gene cut is required for the mitotic cycle/endocycle switch and cell differentiation in Drosophila follicle cells. Development *132*, 4299-4308.

Takashima, S., Paul, M., Aghajanian, P., Younossi-Hartenstein, A., and Hartenstein, V. (2013). Migration of Drosophila intestinal stem cells across organ boundaries. Development *140*, 1903-1911.

Terhzaz, S., Finlayson, A.J., Stirrat, L., Yang, J., Tricoire, H., Woods, D.J., Dow, J.A., and Davies, S.A. (2010). Cell-specific inositol 1,4,5 trisphosphate 3-kinase mediates epithelial cell apoptosis in response to oxidative stress in Drosophila. Cell Signal *22*, 737-748.

Veenstra, J.A., Agricola, H.J., and Sellami, A. (2008). Regulatory peptides in fruit fly midgut. Cell Tissue Res *334*, 499-516.

Wallrath, L.L., Burnett, J.B., and Friedman, T.B. (1990). Molecular characterization of the Drosophila melanogaster urate oxidase gene, an ecdysone-repressible gene expressed only in the malpighian tubules. Mol Cell Biol *10*, 5114-5127.

Wang, J., Kean, L., Yang, J., Allan, A.K., Davies, S.A., Herzyk, P., and Dow, J.A. (2004). Function-informed transcriptome analysis of Drosophila renal tubule. Genome Biol *5*, R69.

Witzgall, R., Brown, D., Schwarz, C., and Bonventre, J.V. (1994). Localization of proliferating cell nuclear antigen, vimentin, c-Fos, and clusterin in the postischemic kidney. Evidence for a heterogenous genetic response among nephron segments, and a large pool of mitotically active and dedifferentiated cells. J Clin Invest *93*, 2175-2188.

Wu, L.H., and Lengyel, J.A. (1998). Role of caudal in hindgut specification and gastrulation suggests homology between Drosophila amnioproctodeal invagination and vertebrate blastopore. Development *125*, 2433-2442.

Xu, K., Liu, X., Wang, Y., Wong, C., and Song, Y. (2018). Temporospatial induction of homeodomain gene cut dictates natural lineage reprogramming. Elife *7* e33934.

Yang, M.Y., Wang, Z., MacPherson, M., Dow, J.A., and Kaiser, K. (2000). A novel Drosophila alkaline phosphatase specific to the ellipsoid body of the adult brain and the lower Malpighian (renal) tubule. Genetics *154*, 285-297.

Yu, H.H., Chen, C.H., Shi, L., Huang, Y., and Lee, T. (2009). Twin-spot MARCM to reveal the developmental origin and identity of neurons. Nat Neurosci *12*, 947-953.

Zhou, L., Schnitzler, A., Agapite, J., Schwartz, L.M., Steller, H., and Nambu, J.R. (1997). Cooperative functions of the reaper and head involution defective genes in the programmed cell death of Drosophila central nervous system midline cells. Proc Natl Acad Sci U S A *94*, 5131-5136.

Zielke, N., Korzelius, J., van Straaten, M., Bender, K., Schuhknecht, G.F.P., Dutta, D., Xiang, J., and Edgar, B.A. (2014). Fly-FUCCI: A versatile tool for studying cell proliferation in complex tissues. Cell Rep *7*, 588-598.

Figure Legends

Figure 1. **Adult *Drosophila* renal stem cells reside in the ureter and lower tubules**

(A) Drawing showing an adult *Drosophila* Malpighian tubule with its connection at the midgut (MG)/hindgut (HG) junction. Stem cell zone (purple) comprises the ureter and lower tubules, upper tubules (yellow) consist of main segment, transitional segment and initial segment. Renal stem cells (red), principal cells (blue) and stellate cells (green) are indicated. (B) Drawing of cross section of the ureter (left) and lower tubule (right). RSC: renal stem cell; BM: basement membrane; PC: principal cell; CM: circular muscle; LM: longitudinal muscle.

(C) An electron micrograph showing a cross section of the lower tubule. An RSC is pseudocolored in pink. Enlarged micrographs depicting the morphology of mitochondria (denoted by yellow arrow) in RSC and principal cell are shown in (C1) and (C2), respectively. (D) Z-stacked immunofluorescence micrograph of the ureter and lower tubules from a 3-day old *esg-Gal4 > UAS-myrRFP* female. The lower ureter containing smaller PCs joins with the upper ureter containing large PCs as indicted by a dotted line. Regions of both D1 and D2 are shown at high magnification on the right. red = RFP; green=anti-Cut; blue = DAPI. Note relatively weak staining of Cut was seen in RSCs (denoted by yellow asterisks). (E) A cross section view of lower tubule. RSCs are indicated by arrows. (F) Graph summarizing the relative numbers of the major cell types in the ureter and lower tubules. PC_s : small principal cells located at the lower ureter; PC_l: large principal cells located at the upper ureter and lower tubules. (G) Plot of nuclear volume of the indicated cells from the stem cell zone, showing differences that strongly correlate with ploidy. (H) Box plot showing the number of RSCs (marked by esg>RFP) per pair of Malpighian tubules in 3,14,30,50 and 60 -day-old animals.

Figure 2. Single cell gene expression of the SCZ in adult Malpighian tubule

(A) t-Distributed Stochastic Neighboring Embedding (tSNE) plot of tubule cells in the SCZ of adult Malpighian tubules. (B) Cell types are identified based on differentially expressed marker genes. (C) Violin plots showing the expression of selected genes among the six cell types. (D). Immunostaining of Dl showing Dl is expressed in RSCs. (E) Immunostaining of the Notch extracellular domain (NECD) showing Notch is expressed in RSCs. (F) Immunofluorescence micrograph showing NRE-GFP is barely detectable in adult Malpighian tubules. (G) Quantification of percentage of RSCs that express Dl, Notch and NRE-GFP, respectively. Data are means± SD, n=10-11 animals.

(H) Expression of Df31-GFP is highly enriched in RSCs. (I) Expression of *cad* visualized using *cad-Gal4* driven UAS-RedStinger expression.

Figure 3. RSCs only respond to damage near the SCZ

(A-C) Ablation of PC in the SCZ by forced expression of *rpr,hid* with *c507-Gal4*^{ts} induced regeneration. Control in (A). Expression of *UAS-rpr, hid* with *c507-Gal4*^{ts} for 7 days ablated preexisting PCs in the SCZ (B). Recovery at 18^{o}C for 21 days (C). (D) Quantification of nuclear volume of preexisting PCs and replacement PCs in the SCZ from control animals and recovered animals, respectively. Bar denotes the average value. (E) Schematic drawing depicting the surgical procedures to remove part of Malpighian tubules. One of the anterior pair of Malpighian tubules can be severed in the upper tubule region or in the lower tubule, while the other intact Malpighian tubule serves as control. Surgical sites in (F-J) are shown by dashed lines. (F-H) Examples of surgical removal of Malpighian tubules from *esg-Gal4,UAS-myrRFP* female adults

at different sites followed by 2 days EdU feeding. (F) Surgical injury in the lower tubule promoted EdU incorporation into *esg>RFP*$^{+}$ RSCs near the surgical site. (G) Surgical injury in the upper tubule 5 PCs away from the SCZ slightly increased EdU incorporation in the RSCs at the most distal SCZ. (H) Surgical injury in the upper tubule 10 PCs away from the SCZ did not increase EdU incorporation in the RSCs.

(I-J) Lineage tracing of RSCs after surgery. *Act<STOP<lacZ* tracer flies were crossed to *esg-Gal4,UAS-flp,UAS-myrRFP; tub-Gal80*^{ts} driver flies at 18^{o}C. 3-7 day old female progeny with proper genotype were subject to the surgical procedures and were subsequently shifted to 29^{o}C for lineage analysis. (I) Injury in the lower tubule led to significant formation of new tubule cells derived from RSCs. (J) Injury in the upper tubule (about 10 principal cells away from SCZ) did not promote formation of new tubule cells. (I') and (J') are enlarged images corresponding to the dashed box in (I) and (J) respectively.

Figure 4. Damage activates Notch signaling which in turn regulates differentiation of RSCs

(A) NRE-GFP staining was used to indicate Notch signaling activity. Expression of NRE-GFP is barely detectable in the SCZ under normal conditions. In contrast, surgical resection of a Malpighian tubule induced the expression of NRE-GFP near the surgical site (indicated by red triangle). (B) Expression of Cut is upregulated in the esg>RFP+ cells around the surgical site (red triangles) compared to esg>RFP+ cells in the intact Malpighian tubules (indicated by yellow arrowhead). (C-D) Lineage analysis of Notch-depleted RSCs following surgical resection of Malpighian tubule. Expression of N^{RNAi} driven by *esg*^{ts} for 14 days resulted in accumulation of RSCs near the surgical site. (E-H) MARCM clones showing that *N*^{55e11} mutant cells (F,H)

express Dl and fail to polyploidize and turn on the PC differentiation marker Cut. Control in (E) and (G). (I) Model for quiescent RSC-mediated homeostasis maintenance of the ureter and lower tubules. In normal conditions, RSCs are in a quiescent state. Damage to the ureter and lower tubules promotes the exit from quiescence through upregulation of multiple pathways including JNK, Jak/Stat and EGFR/MAPK etc. Meanwhile, damage also upregulates Notch signaling pathway and which in turn upregulates Cut to ensure that activated RSCs (RSC^{A}) only differentiate into replacement principal cells.

Figure 5. Activated RSCs can undergo both symmetric and asymmetric division upon damage

(A-B) Expression of rpr and hid driven by c507-Gal4ts for 7 days at 29oC was used to genetically ablate PCs in the lower tubules and ureters. (A) Mitotic cells (marked by PH3 staining, green) expressed the RSC marker Dl (red) in regenerating Malpighian tubules.

(B) Mitotic cells (marked by PH3 staining, red) were negative for RB marker NRE-GFP (green) in regenerating Malpighian tubules.

(C-F) Twin-spot MARCM system was used to generate RFP and GFP-labelled twin spots. One day before clone induction, animals with appropriate genotype were subjected to surgical resection of upper tubules to activate the quiescent RSCs.

(C) Predicated twin-spot fates after asymmetric or symmetric division. (D) Example of an RSC/RSC pair of twin spots at day 7 after clone induction. (E) Example showing an RSC/RSC of pair twin spots and an RSC/RB pair of twin spots. (F) Observed percentage of symmetric division and asymmetric division.

Figure 6. RSCs are normally quiescent

(A and B) Phospho-histone H3 (Ser10) (PH3) staining was done to label mitoses in wild-type (A) and *esg-Gal4^{ts} >UAS-upd1* (B) Malpighian tubules. After 6 days of expression of Upd1, mitoses were readily present. Inset: enlarged image of the dashed box showing PH3^{+} cells are esg>RFP^{+} RSCs. (C) Quantification of RSCs proliferation induced by expression of *UAS-upd1*. Data represent means± SD, *** denotes Student's t test $p<0.001$.

(D) Representative image of EdU labeling after 2d in wild type Malpighian tubules. Yellow arrowheads denote esg>RFP+ RSCs labelled with EdU. Insets are enlarged images of dashed boxes. (E) Quantified percentage of EdU-positive RSCs after continuous EdU labeling for 2 days and 4 days, n>10 female flies. (F) Cell cycle phase distribution of RSCs as assessed by FUCCI.

(G-J) MARCM technique was used to generate GFP marked mitotic clones with different heat shock dose. Compared to control (G), there was a significant increase in the GFP marked clones in the midgut but not Malpighian tubules after 2X heat shocks (H); the yellow asterisk denotes the autofluorescence from fecal contents in the rectum. Increased RSC clones were seen with 6X heat shocks (I). As expected, labeling was restricted to the ureter and lower tubules, where RSCs are located. (J) Representative image showing both single cell transient clones (outlined in dashes; the single cell is denoted by yellow arrowhead) and multi-cell RSC clones (outlined in dashes), containing a single Dl^{+} RSC (denoted by red triangle). No Dl^{+} cells were detected in the single-cell transient clones. (K) Representative image of GFP marked clones in the lower tubules showing the differential expression levels of Cut in different cell types in RSC clones (outlined by yellow dashes). Cut is expressed at a low level in a single 2C cell in each clone that is presumably an RSC (white arrows). Downstream cells that are often of higher ploidy show higher Cut expression.

Figure 7. RSCs respond to stone formation

(A) Longitudinal optical section view of the ureter and lower tubules from a wild-type animal.The surrounding muscles and brush borders of principal cells are marked by phalloidin staining (green). (B) Longitudinal section view of the ureter and lower tubules from ry^{506} mutant bearing stones (yellow arrowhead) in tubule lumen. Note that detached principal cells (white arrows) were found in tubule lumen. (C-D) Representative electron micrographs showing stones and cell debris were seen in the ry^{506} lower tubule (D) but not in the control tubule (C). (E) Immunofluorescence image showing that stones were present in only one pair of MTs in the same 14-day-old ry^{506} fly. Supernumerary tubule cells were present in the stones-carrying tubules compared to the stone-free tubules. (F-J) RSCs are essential for ureter and lower tubule repair. Representative images showing that ureter and lower tubules from esg^{ts}>*RFP* flies cultured on normal food (F) and allopurinol food (G) as well as those from esg^{ts}>*RFP*+*Rac1.N17* flies cultured on normal food (H) and allopurinol food (I) for 14 days after eclosion. Flies were shifted to 29°C since late L3 to induce the expression of Rac1.N17. Expression of *Rac1.N17* inhibited formation of RSCs in the ureter and lower tubules and completely blocked allopurinol induced production of supernumerary tubule cells. (J) RSCs-depleted flies showed a shortened lifespan compared to control flies when reared on allopurinol food. ns denotes log-rank test $p > 0.05$, *** denotes log-rank test $p < 0.001$.

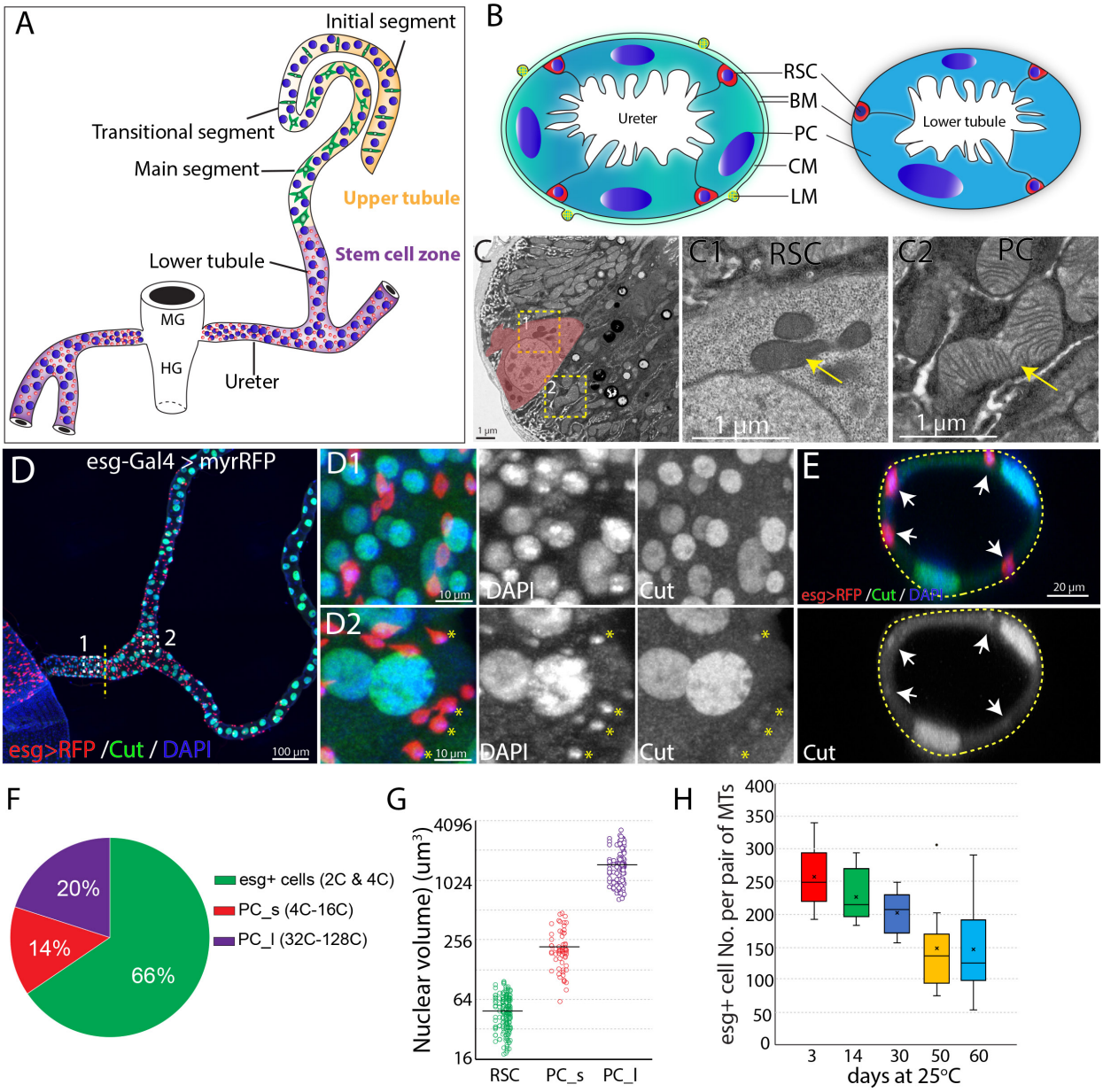

Figure 1

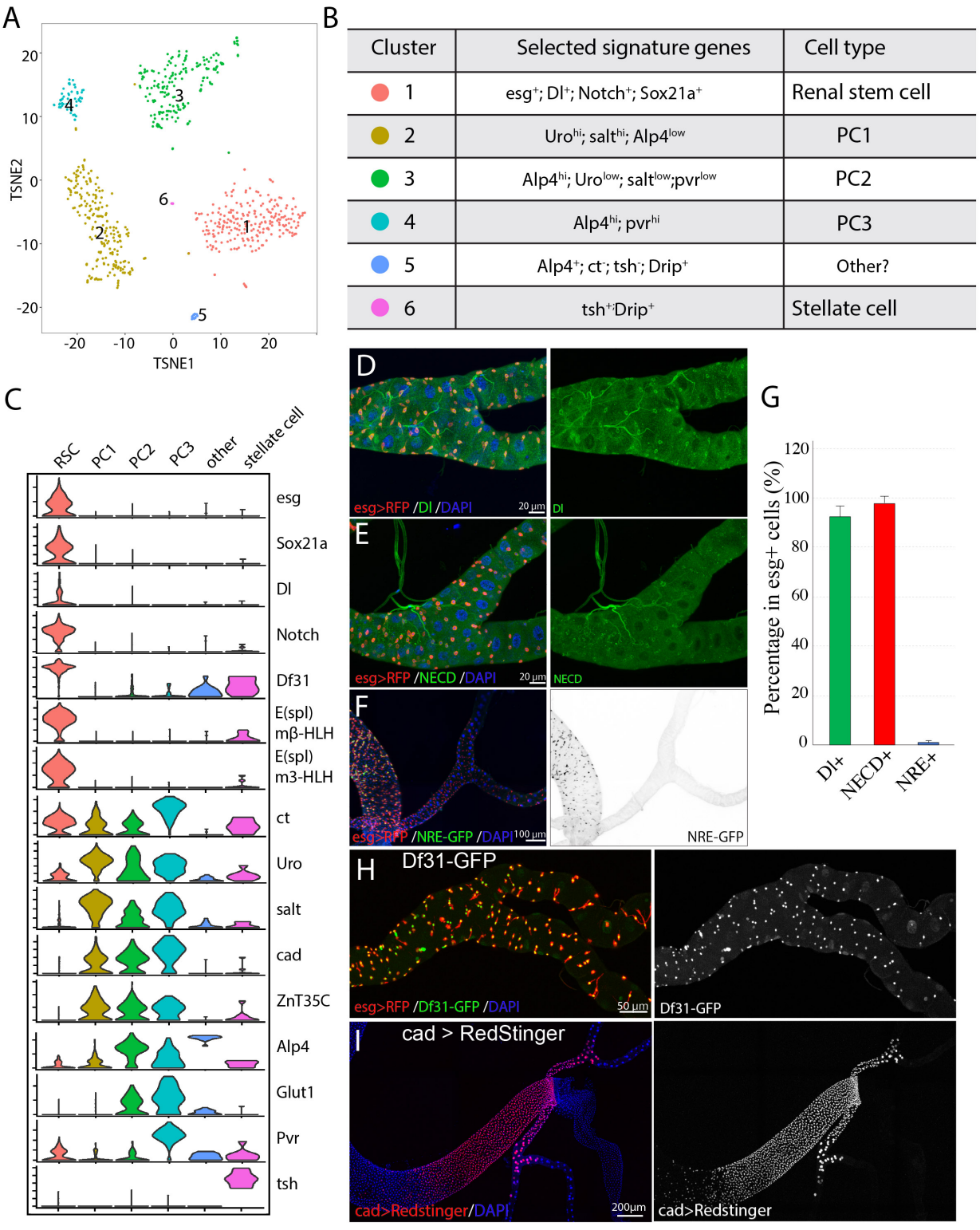

Cluster	Selected signature genes	Cell type
1	esg^{+}; Dl^{+}; Notch^{+}; Sox21a^{+}	Renal stem cell
2	Uro^{hi}; salt^{hi}; Alp4^{low}	PC1
3	Alp4^{hi}; Uro^{low}; salt^{low};pvr^{low}	PC2
4	Alp4^{hi}; pvr^{hi}	PC3
5	Alp4^{+}; ct^{-}; tsh^{-}; Drip^{+}	Other?
6	tsh^{+};Drip^{+}	Stellate cell

Fig. 2

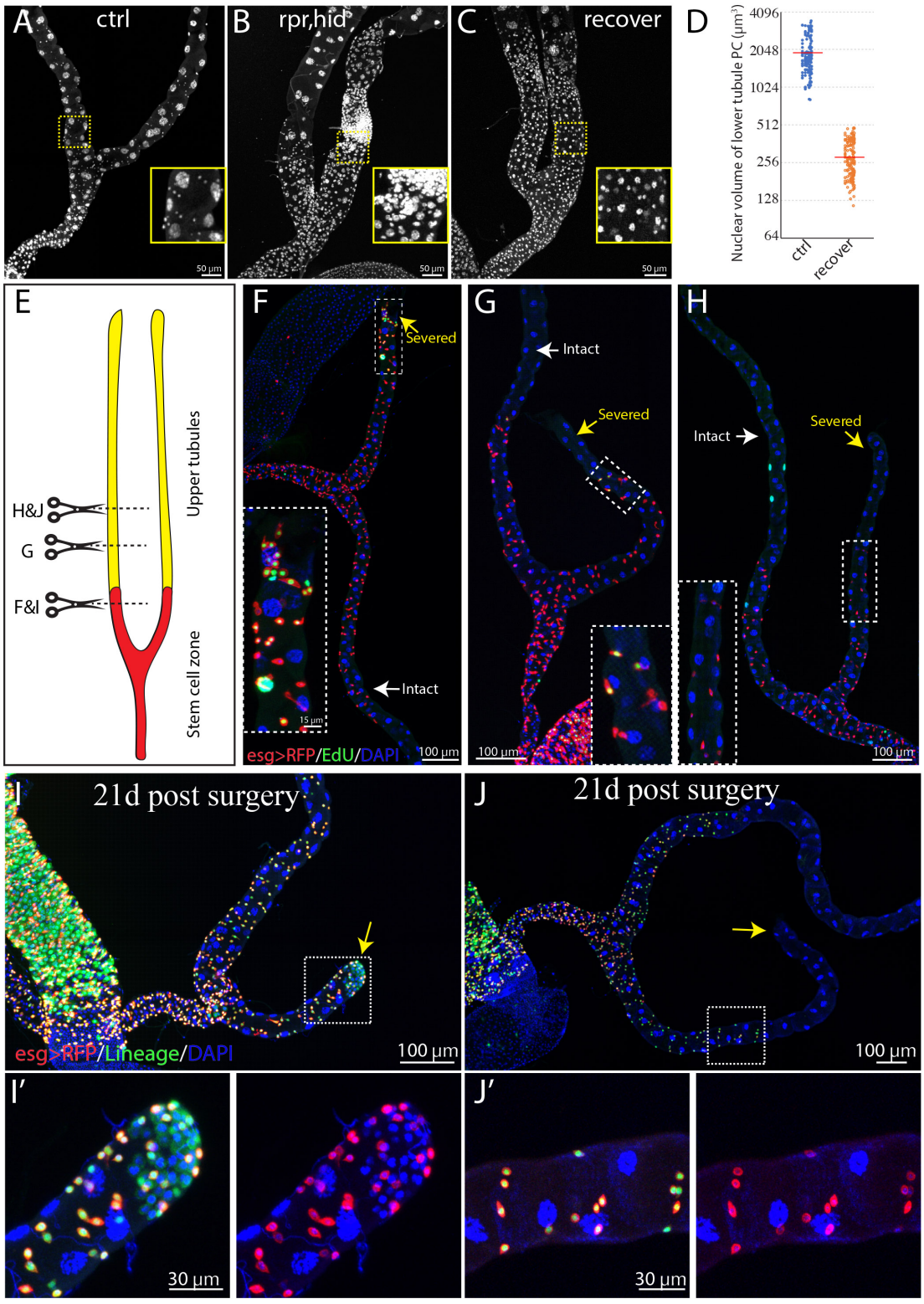

Figure 3

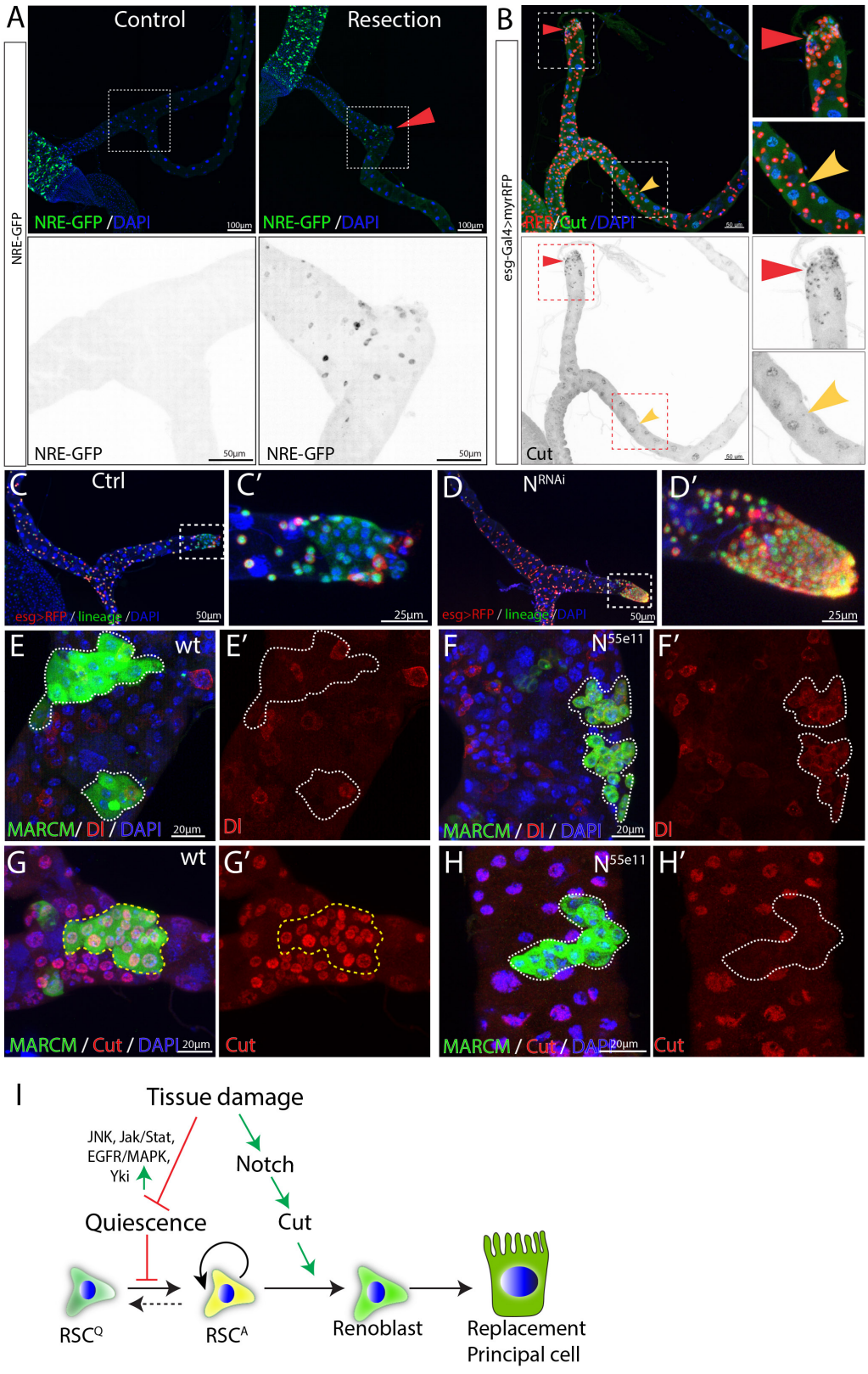

Figure 4

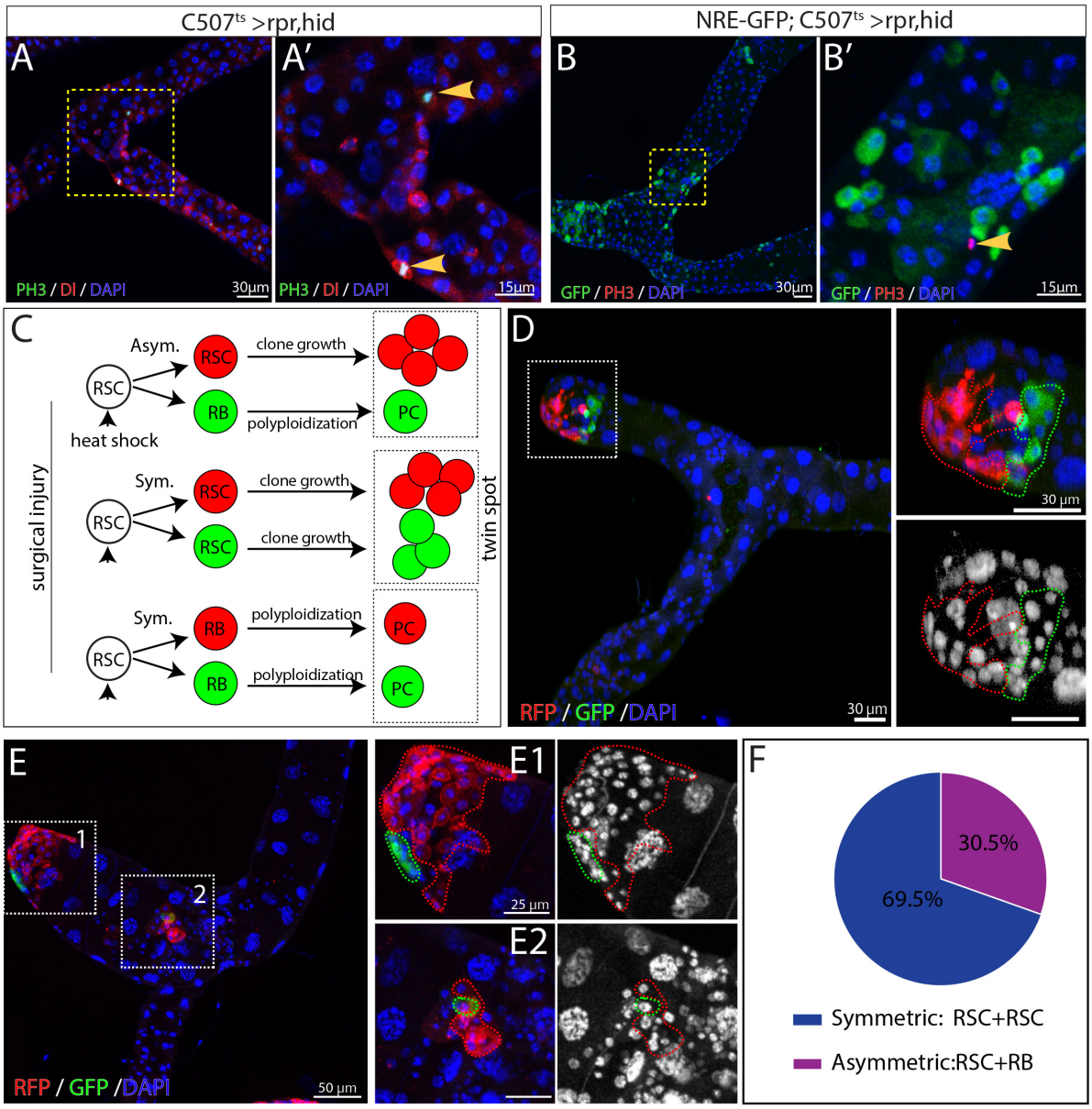

Figure 5

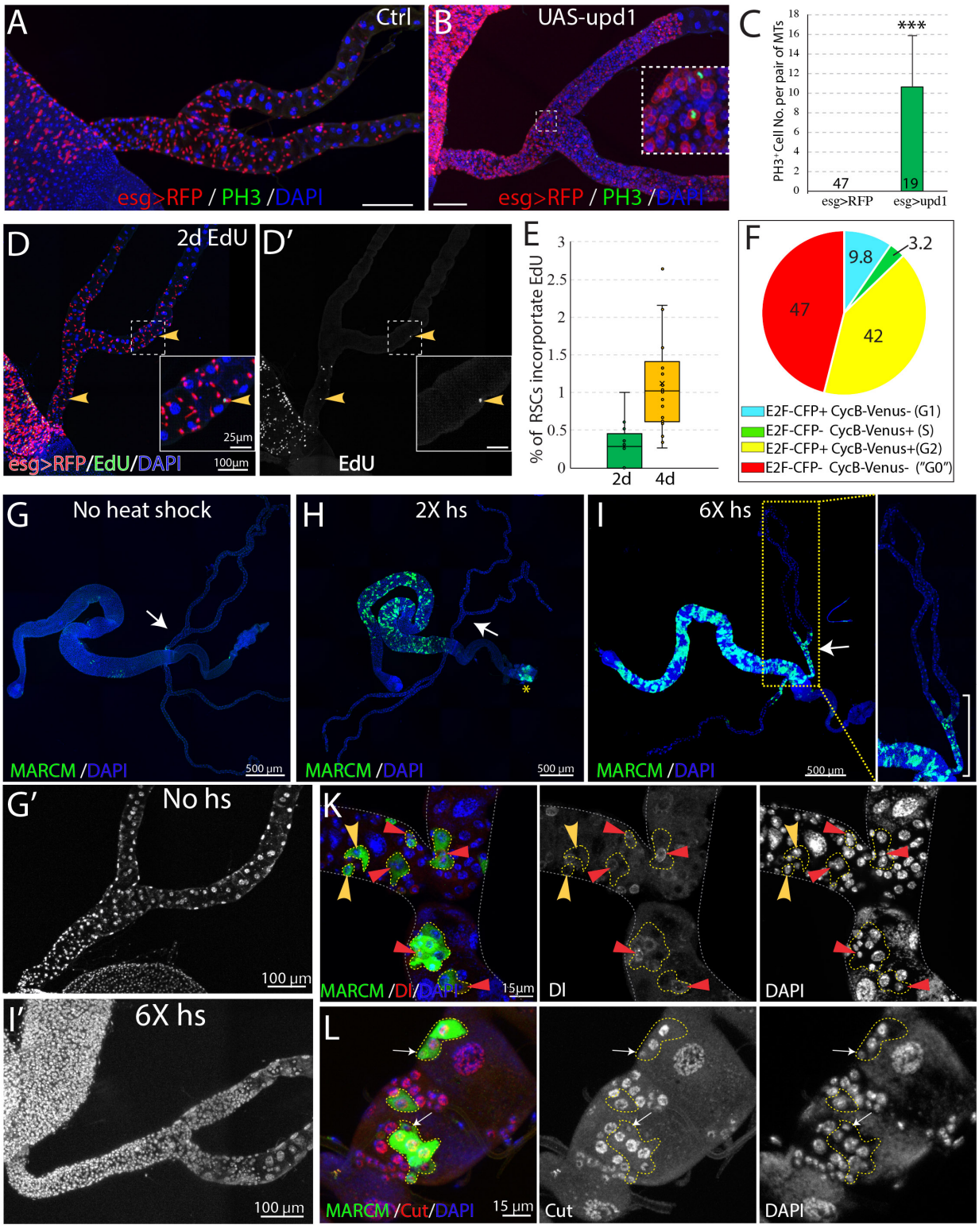

Figure 6

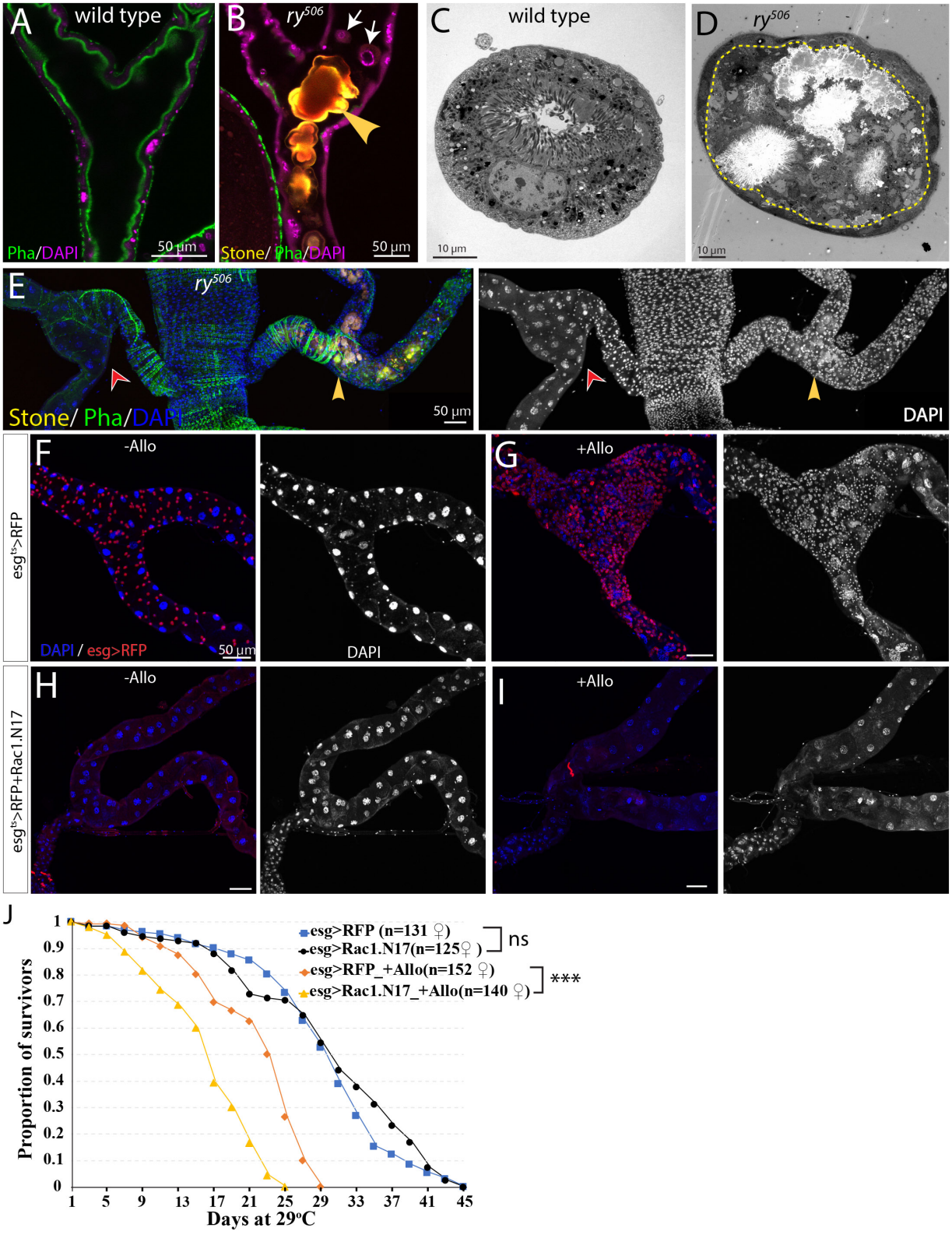

Figure 7